Comparison of the lateral carrier transport between a GaAs single quantum well and the AlGaAs barrier during cathodoluminescence excitation

D. Araújo
Departamento de Ciencia de los Materiales e IM y QI, Universidad de Cádiz, Apartado 40, 11510 Puerto Real, Spain

G. Oelgart
Fachbereich Physik der Universität Leipzig, Linnésstrasse 5, 7010 Leipzig, Germany

J.-D. Ganière and F. K. Reinhart
Institut de Micro-et Optoélectronique, Ecole Polytechnique Fédérale de Lausanne, 1015 Lausanne, Switzerland

(Received 8 September 1993; accepted for publication 1 March 1994)

In a recent paper we measured the lateral hole diffusion in a GaAs/AlGaAs single quantum well (SQW) by a novel method. At helium temperature, we estimate a lateral hole diffusion length in the QW of 1.5 μm. However, the assumption that diffusion takes place mainly in the SQW needs to be checked, as the measured diffusion length is the result of two competing processes: (i) hole diffusion in the SQW plane itself and (ii) hole diffusion in the barrier followed by recombination in the SQW. We present here a comparison between the lateral hole distribution in the SQW and in the AlGaAs barrier. First, we estimate the hole diffusion length in the barrier fitting experimental cathodoluminescence linescans on simulated ones. Second, using the measured diffusion lengths in the QW plane and in the bulk barrier and modeling the carrier transport, we deduce the lateral hole distribution in both layers. It is found that even for very large barriers (1.2 μm), the hole diffusion in the barrier contributes less than 0.1% of the total lateral hole diffusion. The lateral transport is mainly carried by holes in the QW (2D diffusion) due to their confinement in the well.

I. INTRODUCTION

Investigations of transport properties of carriers parallel to heterointerfaces have attracted considerable interest not only due to the related physics but also due to their device application. Mobilities can be obtained by Hall measurements,[1–3] and recombination lifetimes through time-resolved cathodoluminescence measurements[4] and time-of-flight (TOF) measurements.[5–7] To deduce the diffusion length it is necessary to do two complementary experiments. Thus, a direct determination of the diffusion length is very attractive. In this connection, the cathodoluminescence (CL) is very convenient as direct transport measurements taking into account all the diffusion process (single carriers, excitons, ambipolar) are possible. Direct CL carrier diffusion length measurements were performed recently by two different approaches.[8,9]

In previous papers,[10,11] we analyzed the electron-hole (e-h) transitions around grown-in dislocations (GDs) of a single quantum well (SQW) structure grown by metalorganic chemical vapor deposition (MOCVD). The unintentionally doped (Si:$\sim10^{16}$ cm^{-3}) structure, shown in the inset of Fig. 1, consists of a GaAs/$Al_xGa_{1-x}As$ ($x=0.5$) SQW of nominal 20 Å width. The thickness of the GaAs buffer layer and of the AlGaAs barriers amounted to 0.5 and 1.2 μm, respectively. The structure contained GDs that originated at the substrate. As shown in Fig. 1, additional peaks were observed near the GDs from the AlGaAs barrier and from the SQW. We analyzed the free-exciton recombination in the SQW by photoluminescence (PL) and cathodoluminescence (CL). Thickness variations of the SQW, due to the growth peculiarities near the dislocations, were demonstrated using CL micrographs at a selected wavelength at 5 K.[10] Impurities and native defects were also found in these regions around the dislocations in the QW and in the barrier.[11] This local change of the optical properties of the material occurs in a region of about 1 μm around the dislocation. Selecting the CL detection wavelength at the excitonic and/or at impurity related wavelength in the SQW, we determined a total lateral hole diffusion length at helium temperature of 1.5 μm.[9] Such diffusion determination is performed assuming carrier diffusion mainly in the QW.

However, the assumption that the lateral diffusion is mainly in the SQW needs to be checked, as the directly measured diffusion length is obviously the result of two competing processes: (i) the hole diffusion in the SQW plane itself and (ii) the hole diffusion in the barrier followed by a recombination in the SQW. In this paper we compare the contribution of the hole diffusion in the barrier to the hole diffusion in the SQW during beam scan across the dislocation region.

II. EXPERIMENTAL RESULTS AND DISCUSSION

The geometry of the experiment is shown in Fig. 2. 2D and 3D hole diffusion take place in the QW and the AlGaAs barriers, respectively. Therefore, a different lateral hole concentration distribution is expected in the QW and the barrier, because the holes are confined in the QW case. To compare the QW with the barrier hole lateral distribution, we solve the steady state equation for both cases in the Dirac-generation approximation. The diffusion length was measured over a distance of 10 μm for the QW (geometry of Fig. 2) and over a distance of ≈1.2 μm for the barrier (geometry

 0021-8979/94/76(1)/342/5/$6.00

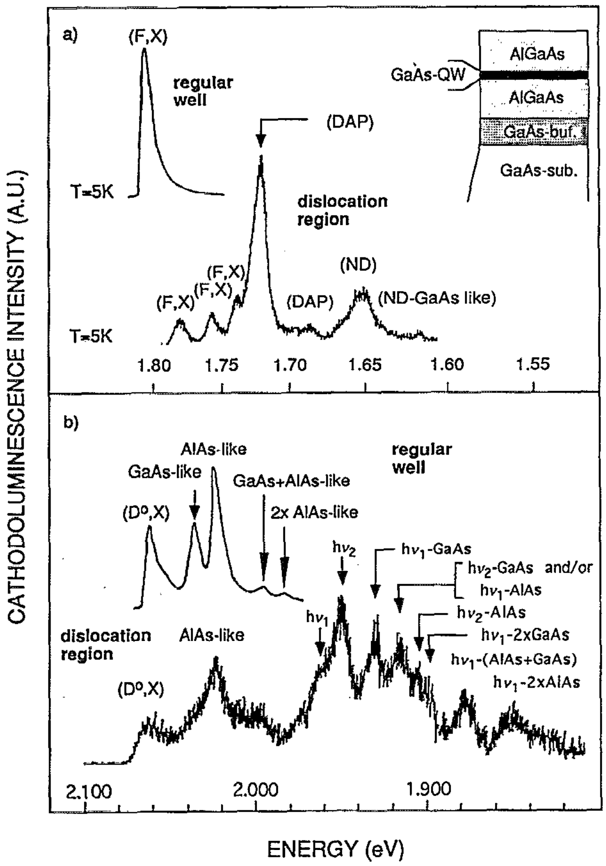

FIG. 1. Cathodoluminescence (CL) spectra on the defects free region (regular region) and around the dislocations. (a) CL spectra corresponding to the GaAs-QW emission, (b) CL spectra corresponding to the AlGaAs-barrier emission.

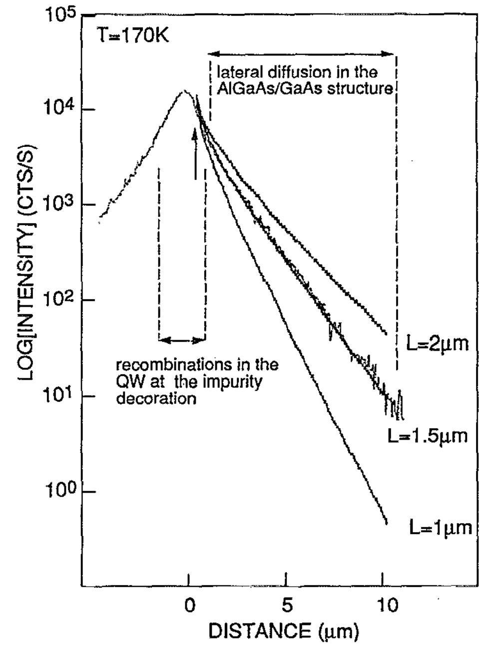

FIG. 3. Calculated and experimental CL profiles across a dislocation region. The calculated curves are fitted for diffusion lengths of 1, 1.5, and 2 μm. The monochromatic experimental CL profile is taken at the native defect energy E_{ND}=1.658 eV and at 170 K. The beam energy and current are E_{pr}=20 keV and I_b=0.5 nA. The inflexion point of both calculated and experimental profiles are shown by the mark.

A. Hole diffusion in the QW

A simple model of carrier diffusion in a cylindrical system should describe the observed CL-intensity profile. For the low injection regime, we can write the steady-state equation for the hole concentration p in the n-doped SQW:

of Fig. 4). Thus, the Dirac-generation approximation is acceptable in the QW measurement, but for the geometry of Fig. 4 comments are necessary to explain the diffusion length measurement.

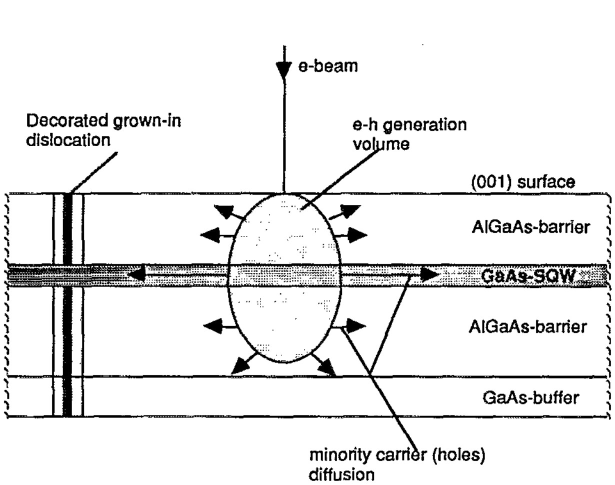

FIG. 2. Geometry of the experiment. The different hole diffusion processes, 3D diffusion in the barrier and 2D diffusion in the SQW are shown.

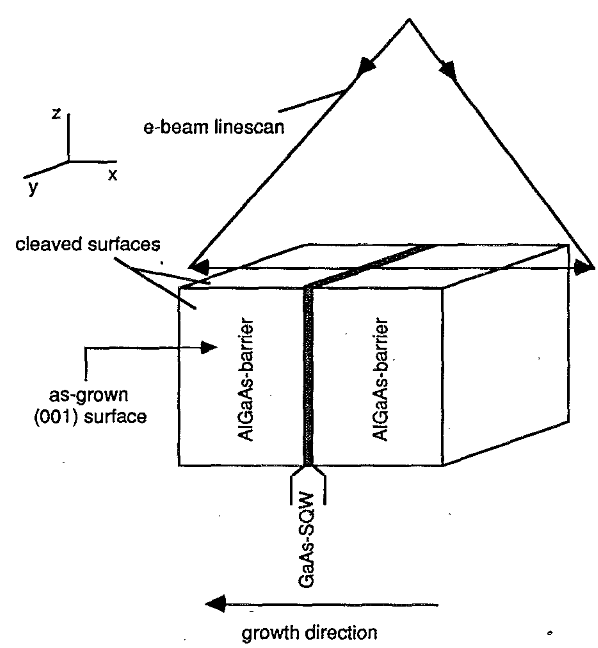

FIG. 4. Schematic representation of the geometry used for the hole diffusion length measurements in the $Al_{0.5}Ga_{0.5}As$ barrier.

$$\frac{\partial p}{\partial t}=0=D\left(\frac{\partial^2 p}{\partial \rho^2}+\frac{1}{\rho}\frac{\partial p}{\partial \rho}\right)-\frac{p}{\tau}+g(\rho), \quad (1)$$

where the first term is the hole diffusion term in cylindrical coordinates. The second term is the recombination rate, and the third one is the generation rate. D and τ are the diffusion constant in (cm^2/s) and the recombination lifetime in (s), respectively.

To simplify Eq. (1), $g(\rho)$ is considered as a Dirac function. Relating ρ with the diffusion length, $L=\sqrt{D\tau}$, we introduce a new variable $r=\rho/L$.

The exact solution of Eq. (1) is

$$p(r)=CK_0(r), \quad (2)$$

where $K_0(r)$ is the modified Bessel function of the second species of zero order (Kelvin function of zero order) and C a constant. The asymptotic development of the solution is

$$p(r)\sim\frac{1}{\sqrt{2\pi r}}\,e^{-r}. \quad (3)$$

To determine the constant C, we consider the carrier flux $F(\rho)$ at the origin must be finite. We find

$$\lim_{\rho\to 0}F(\rho)=\lim_{\rho\to 0}\left(-2\pi\rho D\,\frac{\partial p(\rho)}{\partial \rho}\right). \quad (4)$$

Introducing the solution expressed in (2) and knowing that $\partial K_0(\rho)/\partial\rho=-K_1(\rho)$, we obtain

$$\lim_{\rho\to 0}F(\rho)=\lim_{\rho\to 0}[2\pi C\rho DK_1(\rho)=2\pi CD \quad (5)$$

as

$$\lim_{\rho\to 0}[\rho K_1(\rho)]=1. \quad (6)$$

This carrier flux has to be equal to the excitation rate, G (s^{-1}), in the SQW: $C=G/2\pi D$.

In Fig. 3, in addition to the CL profile at a temperature of 170 K at the native defect (ND) energy (1.658 eV) across a dislocation, the carrier density solution of Eq. (3) is fitted for three different diffusion lengths. The theoretical profile for $L=1.5$ μm is found to fit precisely with the experimental CL profile and therefore confirm a diffusion length value of 1.5 μm in the regular material. The inflexion point (see the mark) on the theoretical curves at $\rho\approx 0.2$ μm corresponds to the inflexion point observed experimentally.

B. The hole diffusion in the $Al_{0.5}Ga_{0.5}As$ barrier

To estimate the lateral concentration of holes in the barrier we first measured the hole diffusion length in the barrier. The CL-intensity profile, on the cleaved surface of the structure and perpendicular to the SQW, permits to estimate the hole diffusion length in the barrier, based on the exponential decrease on both sides of the SQW. In this case the QW is used as a detector to measure the relative carrier concentration in the AlGaAs versus the distance to the e-h excitation.

To have a sufficient lateral resolution, we performed this measurement at $E_b=5$ keV. But in this case, the maximum excitation depth is 0.1 μm and surface recombination at the cleaved (110) surface perturbs drastically the CL decrease on both sides of the SQW. This effect implies an "apparent" hole diffusion length shorter than the "real" one. To overcome this problem we modeled the hole diffusion length for this present CL experiment with the geometry showed in Fig. 4. In the case of the 3D-diffusion, the Eq. (1) becomes

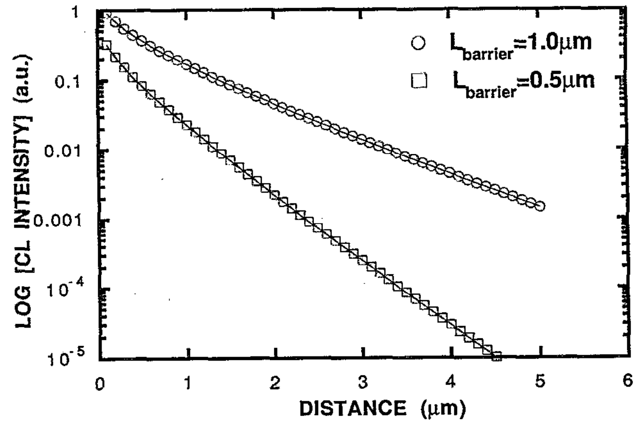

FIG. 5. Calculated CL-intensity profile from Eq. (10) for hole diffusion length in the barrier $L_{barrier}$ of 0.5 μm (open circle) and 1 μm (open squares). The exponential regression [lines passing through the calculated points, see Eq. (11)] gives apparent hole diffusion lengths of 0.44 and 0.82 μm, respectively. The distance in the x axis is the distance of the SQW to the injection point.

$$\frac{\partial p}{\partial t}=0=D\left(\frac{\partial^2 p}{\partial \rho^2}+\frac{2}{\rho}\frac{\partial p}{\partial \rho}\right)-\frac{p}{\tau}+g(\rho), \quad (7)$$

where the first term is the hole diffusion term in spherical coordinates. As for Eq. (1), $g(\rho)$ is considered here as a Dirac function, located in the case of a 5 keV e-beam at 0.1 μm below the (110) surface.[12,13] We consider here the SQW as a detector to measaure the carrier concentration that has diffused from the e-h generation point in the AlGaAs bulk.

To estimate the effect of the surface recombination, we solve Eq. (7) for a surface recombination velocity $S=\infty$. This implies $p(\rho)=0$ at the (110) surface. For this purpose we used a "mirror charge" solution of Eq. (4):

$$p(x,y,z)=\frac{1}{\rho_1}\,e^{-\rho_1}-\frac{1}{\rho_2}\,e^{-\rho_2}. \quad (8)$$

The coordinates ρ_1 and ρ_2 are expressed in cartesian coordinates with the excitation depth of $z_0=0.1$ μm:

$$\rho_1=\frac{\sqrt{x^2+y^2+(z-z_0)^2}}{L_{\text{barrier}}},\qquad \rho_2=\frac{\sqrt{x^2+y^2+(z+z_0)^2}}{L_{\text{barrier}}}. \quad (9)$$

To obtain the total CL intensity of the SQW versus the position it is necessary to integrate the hole concentration on the whole SQW plane:

$$I_{\text{CL}}\propto N(x)=\int_0^{+\infty}\int_{-\infty}^{+\infty}\left(\frac{1}{\rho_1}\,e^{-\rho_1}-\frac{1}{\rho_2}\,e^{-\rho_2}\right)dy\,dz, \quad (10)$$

where I_{CL} is the CL intensity that is proportional to the number of holes, $N(x)$, falling in the SQW. In Fig. 5 we display $N(x)$ as a function of the distance x, i.e., we display the relative CL profile in logarithmic scale. The open circle cor-

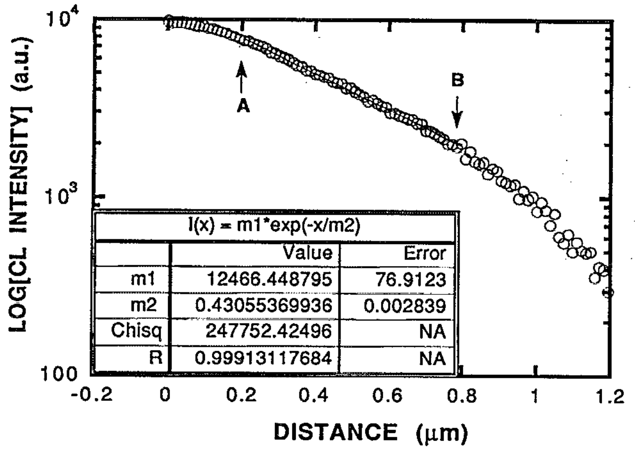

FIG. 6. Measured CL-intensity profile across the SQW at a detection energy of 1.807 eV, a beam energy of 5 keV and a beam current of 0.5 nA. The vertical scale is logarithmic and the distance corresponds to the x axis of Fig. 4. The decrease of the signal leads to an apparent hole diffusion length of $L_{\text{apparent}}=0.43$ μm. This value estimated fitting the experimental points between marks A and B.

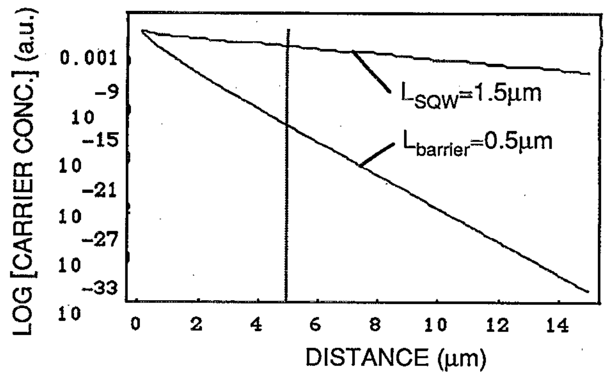

FIG. 7. Lateral hole concentration in the barrier given by Eq. (12) for $L=0.5$ μm and in the SQW given by Eq. (2) for $L=1.5$ μm. The distance correspond to the y axis in Fig. 4.

responds to an AlGaAs bulk diffusion length of 0.5 μm and the open squares to an AlGaAs bulk diffusion length of 1 μm. The exponential regression, shown by a line passing through the point in Fig. 5, gives the "apparent" diffusion length L_{ap}. This value corresponds to the one measured on the experimental CL profile. These regressions are expressed by Eq. (11). The behavior of the hole diffusion for the used beam energy and geometry is

$$N(x)\propto e^{-x/L_{\text{ap}}}. \tag{11}$$

For barrier diffusion length values of $L_{\text{barrier}}=0.5$ and 1.0 μm, we deduce from the fits of Fig. 5, apparent diffusion lengths L_{ap} of 0.44 and 0.82 μm, respectively. Therefore, for a measured barrier diffusion length of 0.44 μm, we must conclude that the real material hole diffusion length is 0.5 μm.

Previous measurements and calculations[14] predict an exponential decrease of the CL profile at low beam energy in spite of the effect of surface recombinations. The surface recombination effect was predicted to only decrease the apparent diffusion length. In Fig. 5, we can observe that the profile, strictly speaking, is no longer exponential. However, the difference is small and we estimate the apparent diffusion length by the fits of Eq. (11). The exponential CL profile is displayed in logarithmical scale in Fig. 6. The observed exponential decrease is shortened at the free (001) surface by surface recombinations and modified near the QW by the generation volume. To estimate the diffusion length, it is then necessary to measure in the middle part of the profile as indicated by the marks A and B. It is impressive that, even for such a thin AlGaAs barrier, a respectable exponential decrease region is observed between the marks. The obtained apparent diffusion length L_{ap} is 0.43 μm. From Fig. 5 and Eq. (11), we conclude that the real hole diffusion length in the AlGaAs barrier is 0.5 μm.

C. Comparison of the hole diffusion in the QW and in the barrier

We will now investigate lateral hole distribution in the barrier compared to the one in the SQW. Equation (7) is still valuable for this 3D diffusion. However, the geometry is different from that one shown in Fig. 4, as we exit from the (001) surface (see Fig. 2).

We make the corresponding assumptions for the carrier concentration estimation in the AlGaAs barrier: (i) as above for the (110) surface but for the QW plane all the carriers that reach the well fall in it, $p(\rho)=0$ at the QW plane, (ii) we neglect the effect of the (001) as-grown surface. The second assumption will make the estimation of the lateral carrier concentration an upper value. In the case of a comparable carrier distribution between the SQW and the barrier, it would be necessary to introduce this term in the equations. As above we also use a "mirror charge" solution:

$$p(x,y,z)=\frac{1}{\rho_3}\,e^{-\rho_3}-\frac{1}{\rho_4}\,e^{-\rho_4}. \tag{12}$$

The holes that diffuse the furthest are generated at the center of the barrier because the carriers generated near the SQW edge or near the (001) surface recombine fast in the SQW or at the surface, respectively. Therefore, we will estimate the lateral concentration of holes in the case of a Dirac generation in the center of the barrier at $z_0=0.6$ μm. In consequence, the obtained lateral hole distribution is obviously an upper estimation. In this geometry, the coordinates ρ_3 and ρ_4 are expressed in Cartesian coordinates as:

$$\rho_3=\frac{\sqrt{x^2+y^2+(z-z_0)^2}}{L_{\text{barrier}}},\qquad \rho_4=\frac{\sqrt{x^2+y^2+(z+z_0)^2}}{L_{\text{barrier}}}, \tag{13}$$

where ρ_4 represents the "mirror" contribution.

In Fig. 7 we display the lateral hole concentration in the barrier and in the SQW. In these fits the hole diffusion lengths are assumed to be 0.5 μm in barrier and 1.5 μm in the SQW as estimated above. The diffusion in the QW follows a law in $r^{-1/2}\exp\{-r\}$ which leads to a larger extension of holes than a law in $r^{-1}\exp\{-r\}$ as in the barrier (where $r=\rho/L$). Thus, in spite of the little difference in the hole diffusion length between the SQW and the barrier, and in spite of the two drastic upper approximations for the lateral carrier diffusion in the barrier, i.e., no (001) surface effects and point generation in the center of the barrier, we have shown that the hole concentration extension is much larger in the case of 2D diffusion. For a precise estimation of the hole diffusion in the barrier, it would be necessary to introduce the spatial dependence of the carrier generation and the (001) surface recombination that would reduce evenmore the estimation of the lateral hole extension in the barrier. However, it is found that the influence of the hole diffusion in the barrier is negligible on the total lateral carrier transport. The calculated hole concentration in the barrier is found to be <0.1% of the one in the SQW at 5 μm from the dislocation.

III. CONCLUSION

In summary, from an independent measurement analysis we estimated a hole diffusion length in the barrier of $L_{\text{barrier}}<0.5$ μm from CL linescan, on the cleaved (110) surface, perpendicular to the SQW. A single model of 3D hole diffusion permits to estimate the lateral hole concentration in the barrier. The comparison with the experimental value of the lateral hole concentration in the SQW showed that the barrier hole diffusion does not contribute significantly to the total lateral hole diffusion. The contribution of this process is found to be less than 0.1% part of the total lateral hole diffusion in the SQW. Thus, we concluded that our direct transport measurements in the SQW are not perturbed by hole diffusion in the barrier. The QW is shown to be a very efficient channel for carrier transport.

ACKNOWLEDGMENT

This work was made possible through grants from the Swiss National Science Foundation (No. 2.979-0.88).

[1] C. Guillemot, M. Baudet, M. Gauneau, A. Regreny, and J. A. Portal, Phys. Rev. B **35**, 2799 (1987).
[2] R. Gottinger, A. Gold, G. Abstreiter, G. Weinmann, and W. Schlapp, Europhys. Lett. **6**, 183 (1988).
[3] H. Sakaki, T. Noda, K. Hirakawa, M. Tanaka, and T. Matsusue, Appl. Phys. Lett. **51**, 1934 (1987).
[4] D. Bimberg, J. Christen, T. Fukunaga, H. Nakashima, D. E. Mars, and J. N. Miller, J. Vac. Sci. Tecnol. B **5**, 1191 (1987).
[5] R. A. Höpfel, J. Shah, P. A. Wolff, and A. C. Gossard, Phys. Rev. B **37**, 6941 (1988).
[6] K. Hattori, T. Mori, H. Okamoto, and Y. Hamakawa, Appl. Phys. Lett. **51**, 1259 (1987).
[7] H. Hillmer, S. Hansmann, A. Forchel, M. Morohashi, E. Lopez, H. P. Meier, and K. Ploog, Appl. Phys. Lett. **53**, 1937 (1988).
[8] H. A. Zarem, P. C. Sercel, J. A. Lebens, L. E. Eng, A. Yariv, and K. J. Vahala, Appl. Phys. Lett. **55**, 1647 (1989).
[9] D. Araújo, G. Oelgart, J.-D. Ganière, and F.-K. Reinhart, Appl. Phys. Lett. **62**, 2992 (1993).
[10] G. Oelgart, L. Lehmann, D. Araújo, J.-D. Ganière, and F.-K. Reinhart, J. Appl. Phys. **71**, 1552 (1992).
[11] D. Araújo, G. Oelgart, J.-D. Ganière, and F.-K. Reinhart, J. Appl. Phys. **74**, 1997 (1993).
[12] J. F. Bresse, Scanning Electron. Microscopy **IV**, 1487 (1982).
[13] G. Oelgart and U. Werner, Phys. Status Solidi A **85**, 205 (1984).
[14] F. Berz and H. K. Kuiken, Solid State Electron. **19**, 437 (1976).